Estuarine, Coastal and Shelf Science 313 (2025) 109075

Contents lists available at ScienceDirect

Estuarine, Coastal and Shelf Science

journal homepage: www.elsevier.com/locate/ecss

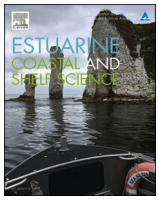

Light and temperature niches of the large benthic foraminifer *Heterostegina depressa*

Chiara M. Duijser [a,1], Rebecca S. van Oostveen [a,1], Elsa B. Girard [a,b], Willem Renema [a,b], Susanne Wilken [a,*]

[a] Institute for Biodiversity and Ecosystem Dynamics (IBED), University of Amsterdam, Science Park 904, 1098XH, Amsterdam, the Netherlands
[b] Naturalis Biodiversity Center, Darwinweg 2, 2333CR, Leiden, the Netherlands

ARTICLE INFO

Dataset link: Light and temperature niches of the large benthic foraminifer Heterostegina depressa (Original data)

Keywords:
Large benthic foraminifera
Heterostegina depressa
Physiology
Micro-CT scanning
Climate change
Thermal niche
Photoacclimation

ABSTRACT

Reef calcifiers, such as symbiont-bearing large benthic foraminifera (LBF), play a major role in shaping (sub) tropical ecosystems. LBF are projected to experience larger fluctuations in light levels as well as elevations in sea surface temperatures, which might be accommodated by a shift in their species distribution towards cooler subtropical regions. While foraminifera are highly sensitive to environmental changes, their light and temperature niches have not been well characterized. Here we examined the ability of the diatom-bearing *Heterostegina depressa* to acclimate to a range of light levels (from 0 to 50 μmol photons m^{-2} s^{-1}) and temperatures (from 15.6 to 33.1 °C) through a 4-week experimental study. Micro-CT scanning of live foraminifera prior to experimental incubations was successfully used to quantify calcification. A thermal niche between 24.4 and 30.3 °C was identified for *H. depressa* based on assessment of growth, calcification and photosynthetic yield. High sensitivity was observed outside this range, as also confirmed by declining photosynthetic efficiency. *H. depressa* showed a light optimum for growth between 25 and 38 μmol photons m^{-2} s^{-1}, and first signs of photoinhibition at 50 μmol photons m^{-2} s^{-1}, while decreased growth was observed in darkness. Acclimatization to higher light intensity is explained by a relative increase in the pigment violaxanthin, as detected by high-performance liquid chromatography (HPLC). Our results suggest that LBF survival could become compromised under future range expansions, however examining the interactive effects of light, temperature, and other environmental stressors on LBF performance are urgently needed as a basis for predicting their responses to future ocean projections.

1. Introduction

Large benthic foraminifera (LBF) play a major role in carbon cycling and sequestration within tropical and subtropical reef ecosystems, contributing approximately 4.8% to the global carbonate production annually (Langer et al., 1997; Hohenegger, 2006; Langer, 2008). They are fundamental in the production of calcareous sediments through the secretion of their calcium carbonate tests, and as a result are vital for reef and beach maintenance (e.g., Hallock, 1981; Yamano et al., 2000; Dawson et al., 2014). Additionally, LBF are widely used as bioindicators on coral reefs, responding rapidly to environmental changes such as ocean warming and eutrophication, thereby offering valuable insights into water quality and ecosystem health (Hallock et al., 2003; Girard et al., 2022).

Similar to corals, LBF engage in symbiotic relationships with eukaryotic and prokaryotic microalgae (i.e., photo-endosymbionts), as well as non-photosynthetic prokaryotes (Lee, 2006; Prazeres and Renema, 2018). Particularly the interaction with photosynthetic algae is crucial for foraminiferal growth, calcification and survival as these symbionts efficiently recycle scarcely available nutrients and supply up to 90% of the energy required by the host (Hallock, 1981, 1985; ter Kuile and Erez, 1991). In addition, photosynthesis and calcification are suggested to mutually enhance each other (Duguay and Taylor, 1978; McConnaughey and Whelan, 1997; Hallock, 2000). Consequently, the LBF are dependent on the intricate relationship with their photosymbiotic algae, shaping their environmental niche. Key requirements include ample light to support the photosynthetic activities of their algal endosymbionts and a suitable temperature range. This suite of conditions confine the biogeographic range of modern-symbiont bearing LBF to (sub)tropical and warm temperate shallow seas (Lee and Anderson,

* Corresponding author.
E-mail address: s.wilken@uva.nl (S. Wilken).
[1] These authors contributed equally to this work.

https://doi.org/10.1016/j.ecss.2024.109075
Received 15 August 2024; Received in revised form 30 October 2024; Accepted 29 November 2024
Available online 30 November 2024

1991; Langer and Hottinger, 2000; Weinmann et al., 2013).

Given these environmental constraints, foraminifera are highly sensitive to environmental change, including ocean warming and alterations in light exposure. A projected global sea surface temperature increase of 4.3 °C by 2100, relative to the years 1850–1900 under the Representative Concentration Pathway 8.5 scenario, poses threats to the algal-host symbiosis and survival of LBF in their current range. This is evidenced by compromised photosynthesis (Schmidt et al., 2011; Uthicke et al., 2012) and reduced growth rates under heat stress conditions (Reymond et al., 2011; Doo et al., 2012). Heat stress can further cause some species (eg. *Heterostegina depressa*) to expel their photosymbionts and thus lead to bleaching (Schmidt et al., 2011), while other species have been reported as very heat-tolerant (eg. *Pararotalia calcariformata*; Schmidt et al., 2016). However, the complete temperature niche is not well characterised for all LBF, and responses to cooler water temperatures (e.g., Fujita et al., 2014) are rarely assessed. The effect of lower temperatures are important since future range shifts could lead to exposure to more seasonal variation, potentially impacting overall LBF health (Langer and Hottinger, 2000; Vergés et al., 2014; Titelboim et al., 2021).

Moreover, LBF are faced with a changing light climate due to alterations in the physical characteristics of reef environments and land-sea interactions, driven by factors such as rising sea levels (Baker et al., 2008), variations in cloud cover (Wild et al., 2011), and anthropogenic activities causing increased levels of terrestrial runoff (Hallock et al., 2006; Prazeres et al., 2016). The anticipated shifts in light availability can significantly impact LBF, with high light intensities leading to increased mortality over a few weeks (Nobes et al., 2008), while darkness causes metabolism to be reduced and a dormancy stage can be triggered (Lintner et al., 2023). This dormancy stage is characterized by short-term inactive life and arrested development within LBF (Ross and Hallock, 2016). However, despite the importance of LBF in reef ecosystems, significant knowledge gaps exist regarding the capacity of foraminifera species to acclimatize to projected temperatures and changes in light exposure.

Here we characterize the light and temperature niches of one of the most abundant LBF species, *Heterostegina depressa*, a crucial step for predicting their responses to future ocean conditions. This diatom-bearing species (Nummulitidae) found in the Indian and Pacific oceans (Hallock, 2000) occurs on rubble and solid substrates throughout the photic zone (Hohenegger et al., 2000; Renema, 2018). It was hypothesized that the physiological responses of *H. depressa* were compromised during heat stress, but also during cold stress. Furthermore, we expected a relatively low light optimum and hence light stress to be observed already at moderate light intensities. To gain a comprehensive understanding of the temperature and light ranges that *H. depressa* can tolerate, it was exposed to a range of light and temperature levels in a 4-week experiment, in which growth, calcification, and photo-physiological characteristics were monitored. Furthermore, to improve methodologies used in a laboratory setting, we applied micro-CT scanning on live specimens before and after the experiment to assess growth, presenting a novel alternative to existing methodologies.

2. Materials and methods

2.1. Specimen collection

Coral rubble was collected from the Indo-Pacific coral reef aquarium in Burgers' Zoo (Arnhem, the Netherlands) in April 2022. Conditions in the coral reef tank are strictly monitored (Janse et al., 2008) and regulated at a salinity of 34.2, pH at 7.9 and temperature of 25–26.5 °C with a seasonal cycle (Janse et al., 2008). Light is year long at a 12:12h day-night cycle. Approximately same-sized (⌀ = 3 mm) *H. depressa* specimens were manually selected based on their homogenous brown coloration, a sign of health. The specimens were left to acclimatize in a small container connected to an air pump and filled with the zoo tank sea water to ambient sampling conditions (24 °C, 70 % humidity and a 12:12 h light-dark cycle) in an incubation chamber (Fitotron®, Weiss Technik, Loughborough, UK). To ensure stable salinity levels during the acclimatization phase, the water levels were monitored and sterile fresh water was added to compensate for evaporation. After three days of acclimatization, all individuals were micro-CT scanned (see below) and transferred to the temperature and light-gradient incubators, in which they were again acclimatized for three days prior to the start of the experiment.

2.2. Experimental set-up

In two experiments, *H. depressa* specimens were incubated for four weeks across either a temperature, or a light-gradient, each consisting of five treatments. The incubation setup consisted of an aluminum frame tightly holding the incubation vials, that was connected to two water baths for temperature control and placed directly above an LED light source. The temperature gradient was created by cooling the frame from one and heating from the other side. The temperature experiment included a range from 8.4 °C below to 9.1 °C above average *in situ* temperature (i.e. 15.6 °C, 18.6 °C, 24.4 °C, 30.3 °C and 33.1 °C; see Supplementary Material Fig. S1A for illustration of the set-up). Prior to starting the incubation, temperatures were decreased/increased gradually by 3 °C per two days. This procedure was chosen to avoid thermal shock and potentially rapid bleaching as has been reported in *H. depressa* within a few days of exposure to 32 °C (Schmidt et al., 2011). However, we note that it might already cause some level of stress prior to reaching the final treatment temperature. In the temperature experiment, specimens were maintained at a constant light level of 12.6 μmol photons m^{-2} s^{-1}. In the light experiment, LBF were exposed to the following light levels: 0, 12.5, 25, 37.5 and 50 μmol photons m^{-2} s^{-1} (Supplementary Material Fig. S1B). In this light-gradient, specimens were maintained at 24 ± 0.1 °C. In both experiments, LBF were maintained at a 12:12 h light-dark cycle with light provided by eight LED lamps covering the range of 380–750 nm (see Supplementary Material Fig. S2 for light spectrum). Each light and temperature treatment consisted of five replicate vials (n = 25), each containing three individuals. Thus, each experiment contained 75 individuals.

Incubations were performed in glass vials (20 mL) containing 16 mL filtered (Nalgene Rapid-Flow™ Filter, 0.2 μm PES membrane, Thermo Fisher Scientific) artificial seawater from the coral reef aquarium in Burgers' Zoo. This seawater (salinity = 34.2, pH = 8.0) was supplemented with 5 mg L^{-1} dried algae provided by Burgers' Zoo as a potential prey, as *H. depressa* has been reported to feed (ter Kuile et al., 1987; Faber and Lee, 1991). Glass vials were closed with a foam stopper to limit evaporation, while still allowing gas exchange. The water level was checked regularly and topped up with Milli-Q water if needed. To prevent biofilm formation, foraminifera were transferred into new vials at the end of each week. All specimens were cleaned with a small brush to remove algae prior to the experiment, which was repeated regularly during the experimental period to prevent algal growth.

In both experiments LBF individuals were micro-CT scanned to determine initial and final shell volumes for all individuals at the experiment's onset and conclusion. Calcification rates were determined in week 2 and 4 using the alkalinity anomaly technique. Photosynthetic efficiency was measured weekly through pulse amplitude modulated (PAM) fluorometry, yet slightly different approaches were used for the temperature and light experiments (see below). In the temperature experiment, photographs were taken of all individuals on a Leica MZ12.5 Stereo Microscope (Leica Microsystems, Wetzlar, Germany) at the end of the four week period to examine changes in coloration. Lastly, pigment concentrations, including chlorophyll *a*, were determined at the end of the light experiment.

2.3. Micro-CT scanning

At the start and upon termination of the experiment, all foraminiferal specimens (n = 150) were scanned using a high-resolution micro X-ray computed tomography scanner (Xradia 520 Versa; Zeiss, Oberkochen, Germany) at Naturalis Biodiversity Center. Individuals were carefully placed inside plastic tubes containing seawater and low-density plastic foil to prevent movement and physical contact between specimens. Each individual was positioned along the inner wall of the tube to ensure optimal visibility during scanning. Within each tube, the specimens were arranged in two distinct horizontal levels, with three individuals per level, allowing simultaneous scanning of six individuals. All specimens were then scanned in a 360° rotation and imaged at 60 kV using a 0.4 magnification objective at a voxel size of approximately 7 μm. Visualization of the calcareous tests through 3D models were generated using Avizo Lite 2020.3.1 3D software (ThermoFisher Scientific, Waltham, MA, United States; see Supplementary Material Fig. S3 for an example). To estimate growth, change in shell volume (ΔV) was calculated from the initial and final volumes. To minimize background noise, the masking operation in Avizo™ Lite was used. For comparability and to avoid bias between the two time points, masking density range was set at 120–255 for all specimens (Supplementary Material Fig. S3). Due to a technical issue, one scan for temperature and 16 specimens for the light treatment were removed from the dataset. Lastly, specimens were divided into three size categories: small 0.465–0.912 mm^3, medium 0.913–1.359 mm^3 and large 1.360–1.806 mm^3, and differences in ΔV within both temperature and light experiments were analyzed.

Given the observed shell breakage during the experiment, where chamberlets and, in some cases, rows of chamberlets (partly) broke off in certain specimens despite careful handling, an assessment of fragility across treatments was conducted. To this end, individuals were classified into two categories: A) Not broken, B) Broken (Fig. 1), and distribution of these categories across treatments was assessed. Notably, one specimen at 33.1 °C was accidently broken in half during PAM-measurement at week 4. This specimen was however, along with all other broken specimens, not excluded from the analyses since it gives valuable information about the fragility of the shell and was still able to photosynthesize.

2.4. Alkalinity anomaly technique

The amount of calcium carbonate ($CaCO_3$) precipitated over the duration of week 2 and 4 of the experiments was measured using the alkalinity anomaly technique (Smith and Kinsey, 1978). During the precipitation of 1 mol $CaCO_3$, 2 mol of bicarbonate (HCO_3^-) are consumed, decreasing total alkalinity (TA) by 2 mol (Smith and Key, 1975; Zeebe and Wolf-Gladrow, 2001). Changes in TA can thus be used to determine net calcification rates. From the culture medium, water samples (5 mL) were taken and filtered (0.2 μm) at the start and end of week 2 and 4, and the alkalinity was measured by titration with 0.1M HCl using an automatic titrator (DMS Titrino 716, Metrohm, Switzerland). Corrections for the effect of nutrient uptake were based on the nutrient-H^+-compensation principle (under the constraint of electroneutrality described by Wolf-Gladrow et al., 2007). To this end, nutrients (nitrate, nitrite, phosphate and ammonium) were analyzed from a filtered (0.2 μm) water sample (10 mL) on an AutoAnalyzer with a 3x dilution (San++, Skalar Analytical B.V., Breda, The Netherlands).

2.5. PAM-fluorometry

For the temperature experiment, effective quantum yield of photosystem II (Y(II)) was measured at the end of each week. Prior to each measurement, any algae present were removed, to prevent interference from algal biomass. The measurements were made directly in the incubation vials at least 30 min after the start of the photoperiod. Effective photochemical quantum yield of PSII is defined as follows (Genty et al., 1989):

$$Y(II) = \frac{F'_M - F'}{F'_M} \quad (1)$$

Fluorescence was measured during exposure to actinic light (F'), while maximum fluorescence levels (F'_M) were measured after application of a saturating light pulse, both using standard settings of a Junior-PAM fluorometer with a 2-mm fiber optic cable (Walz GmbH, Effeltrich, Germany).

For the light experiment, rapid light curves were collected weekly, to get additional information on potential acclimation to different light levels. In week 1 measurements were only performed on individuals in light treatments 12.5, 25 and 50 μmol photons m^{-2} s^{-1} (see Supplementary Material Table S1 for exact sample sizes). All individuals were dark-adapted for 30 min, for measurements of maximum quantum yield in darkness. Rapid Light Curves were then obtained using a Water-PAM (Walz GmbH, Effeltrich, Germany) and the WinControl software (Walz). Foraminifera were subjected to nine increasing light levels for 1 min each (0, 7, 10, 16, 23, 32, 44, 72 and 103 μmol photons m^{-2} s^{-1}). Relative electron transport rate (ETR) was estimated by multiplying quantum yield of photosystem II with each light intensity (PAR). A photosynthesis-irradiance curve was fitted to these data using equation (2) (Eilers and Peeters, 1988) with the fitModel function in R (version 4.2.1; RStudio Team, 2020).

$$rETR = \frac{PAR}{A \cdot PAR^2 + B \cdot PAR + C} \quad (2)$$

Then, the following parameters were derived from these light curves: maximum electron transport rate (ETR_{max}; equation (3)), initial slope (α; equation (4)), minimum saturation irradiance (E_k; equation (5)) and

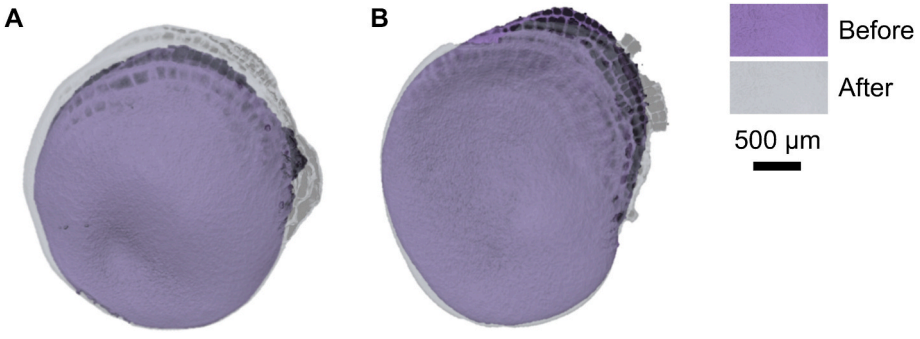

Fig. 1. Classification of foraminifera shells. Specimens labeled as A) "Not broken", and B) "Broken", where the specimen experienced breakage during the experiment due to handling issues or treatment effects. The purple shade refers to the foraminiferal shell before the start of the experiment and is situated underneath the grey shade, which shows the shell's condition at the end of the experiment. Shells that appear as dark purple have been broken, while areas solely in grey denote newly added shell structures. (For interpretation of the references to color in this figure legend, the reader is referred to the Web version of this article.)

optimal intensity (I_m; equation (6); Eilers and Peeters (1988)).

$$ETR_{max} = \frac{1}{B + 2\cdot\sqrt{A\cdot C}}; \quad (3)$$

$$\alpha = \frac{1}{C} \quad (4)$$

$$E_k = \frac{C}{B + 2\cdot\sqrt{A\cdot C}} \quad (5)$$

$$I_m = \sqrt{\frac{C}{A}} \quad (6)$$

2.6. Pigment analysis

At the end of the light experiment and after CT-scanning, all foraminifera were frozen and preserved at −80 °C. Samples were freeze-dried and weighed prior to pigment extraction. Concentrations of chlorophyll *a* (Chl *a*) and accessory pigments associated with light harvesting and photoprotection were determined using high-performance liquid chromatography (HPLC). For this, a modification of the method described by Mantzouki et al. (2018) and Van der Staay et al. (1992) was used. For extraction, 0.5 mm beads and 400 mL of 90% acetone were added to each sample. After two 1-min rounds on a bead-beater, samples were sonicated for 10 min in ice water. A mixture (200 μL) of 7.7% ammonium acetate and 1.5% tributyl ammonium acetate in MilliQ was added to each sample to facilitate pigment binding. Samples were vortexed for approximately 10 s and then centrifuged at 15,000 rpm for 3 min. From the resulting supernatant, 70 μl was used for the analysis on a Shimadzu HPLC (Thermo Scientific, Waltham, MA, United States) as described before (Wilken et al., 2014).

2.7. Statistical analysis

Significant differences in physiological parameters, for which measurements were performed weekly (photosynthetic yield in temperature experiment and light curve parameters in light experiment), were tested using linear mixed models with a repeated measures design and unstructured covariance in SPSS. For photosynthetic yield measurements in the temperature experiment time was included as an additional random factor. For pairwise comparison of main effect (light or temperature) levels Bonferroni adjustment was used. All other statistical analyses were performed using R, with graphical representations produced using the *ggplot2* package (Wickham, 2009). For parameters with less than weekly measurements (growth, calcification, pigment content) one-way analysis of variance (ANOVA) was used, in case the assumptions were met. Tukey's Honestly Significant Difference (HSD) was performed as a post-hoc test using the built-in R function TukeyHSD. In instances where the normality assumption for one-way ANOVA was violated or outliers were detected, the Kruskal-Wallis test from the *rstatix* package was performed as a non-parametric alternative (Kassambara, 2020). Post-hoc pairwise multiple comparisons were conducted with the Dunn test (p-value adjustment method: Benjamini-Hochberg) after a significant Kruskal-Wallis test result (Dunn, 1964; Benjamini and Hochberg, 1995; Kassambara, 2020). In cases where only the homogeneity of variances assumption was violated, Welch's ANOVA within the *rstatix* package was carried out (Kassambara, 2020). Whenever both the assumption of normality and homogeneity were violated, a robust ANOVA (One-Way Trimmed Means Comparisons) was performed with a Lincon post-hoc test from the *WRS2* package in R (Mair and Wilcox, 2020).

3. Results

3.1. Micro-CT scanning

Changes in shell volume observed by micro-CT scanning (further referred to as growth) ranged from −0.255 to 0.454 mm^3 across all specimens in both the temperature and light experiments (Fig. 2). Even within treatments, a high degree of variability in growth was observed.

In the temperature experiment, we found the optimum temperature for growth to be 24.4 °C indicated by a positive change in shell volume (ΔV) in 12 out of 15 individuals (Fig. 2). Both 24.4 °C and 30.3 °C treatments showed significantly higher ΔV compared to the other temperature treatments (Lincon post-hoc test, $p < 0.05$). Five foraminifera at 24.4 °C and seven individuals at 30.3 °C showed a positive ΔV despite having a broken shell, suggesting either thickening of the shell, repair of broken fragments and/or addition of new chamber rows. While the proportion of broken shells did not differ significantly among temperatures (one-way ANOVA, $F(4,20) = 2.12$, $p = 0.116$), specimens at 15.6 °C, 18.6 °C and 33.1 °C were unable to repair broken shell fragments ($\Delta V < 0$).

In the light experiment, foraminifera were able to grow ($\Delta V > 0$) across all light intensities, except under dark conditions (Fig. 2) (Dunn test, adjusted $p < 0.05$). Change in shell volumes increased with higher light irradiances until 37.5 μmol photons $m^{-2}\,s^{-1}$, however, ΔV did not differ significantly between the four light treatments (Dunn test, adjusted $p > 0.12$). Changes in ΔV between the control treatment in the temperature experiment (maintained at 12.6 μmol photons $m^{-2}\,s^{-1}$) were similar to ΔV observed in the control of the light experiment (12.5 μmol photons $m^{-2}\,s^{-1}$; average of 0.064 and 0.085 mm^3, respectively). Furthermore, there were no significant differences in the fraction of broken specimens among light treatments (one-way ANOVA, $F(4,20) = 0.60$, $p = 0.668$). However, specimens under dark conditions exhibited the highest incidence of breakage (8 out of 14; 57.1 %), with least breakages at 12.5 μmol photons $m^{-2}\,s^{-1}$ (4 out of 11; 36.4 %).

3.2. Alkalinity anomaly technique

In week 2 of the temperature experiment, foraminifera incubated at the control treatment were the only ones exhibiting positive precipitation of $CaCO_3$, contrasting with negative values in all other treatments indicating shell dissolution (Fig. 3). The precipitation of $CaCO_3$ was significantly higher in the control than in the 18.6 °C and 33.1 °C treatments (Dunn test, adjusted $p = 0.012$ and $p = 0.006$, respectively). In week 4, all treatments including the control, showed a negative average $CaCO_3$ precipitation. Only two of the five replicates demonstrated calcification in the control, either by forming new chambers or thicker shells. In both weeks, precipitation of $CaCO_3$ was most negative in the highest temperature treatment, although not significant in week 4 (One-Way Trimmed Means Comparisons, $F(4,4.01) = 4.37$, $p > 0.05$).

In the light experiment, highest $CaCO_3$ precipitation occurred consistently at 25 μmol photons $m^{-2}\,s^{-1}$ (Fig. 3). This difference to other light intensities was significant compared to both 0 and 12.5 μmol photons $m^{-2}\,s^{-1}$ in week 2 (Tukey-Kramer, $p = 0.03$, $p = 0.050$), while in week 4 individuals exposed to both 25 and 37.5 μmol photons $m^{-2}\,s^{-1}$ showed significantly higher calcification rates compared to those in darkness (Tukey-Kramer, $p = 0.025$, $p = 0.025$).

3.3. PAM-fluorometry

In the temperature experiment, a decline in photosynthetic yield was observed over time for the two most extreme temperature treatments (15.6 °C and 33.1 °C) and less strongly at 18.6 °C, while it remained stable for the control and 30.3 °C treatments (Fig. 4A). Comparison between temperature treatments revealed the decline in yield to be significant in the lowest temperature compared to 24.4 °C ($p = 0.047$, Supplementary Material Table S2), and also in the highest temperature

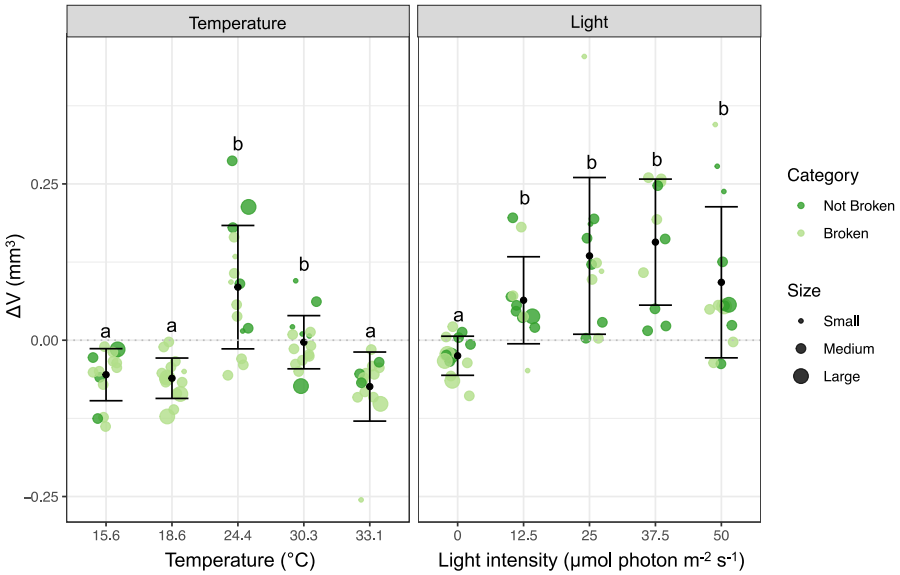

Fig. 2. Change in volume (ΔV) of the calcium carbonate shells per treatment for all individual foraminifera. Colors indicate foraminifera with intact or broken shell. The size of the jitter dots refers to three size categories based on shell volume, i.e., small 0.465–0.912 mm^3, medium 0.913–1.359 mm^3 and large 1.360–1.806 mm^3. One specimen was accidently broken in half during PAM-measurement at week 4 which is the outlier present at 33.1 °C ($\Delta V = -0.26\ mm^3$). While jitter dots thus indicate individual foraminifera, values were averaged per vial (as independent replicate) for statistical analysis. Error bars indicate the mean ± standard deviation. Significant differences between treatments are denoted by a different letter ($p < 0.05$). (For interpretation of the references to color in this figure legend, the reader is referred to the Web version of this article.)

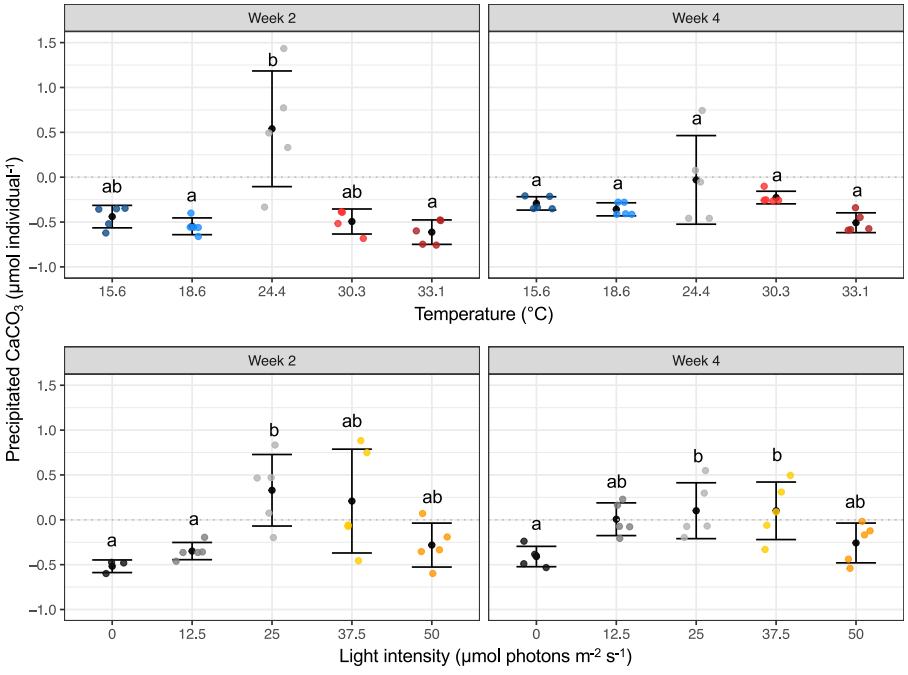

Fig. 3. Precipitated $CaCO_3$ per individual in both the temperature and light experiment. Two measurements are missing in light treatment 0 µmol photons m^{-2} s^{-1} in week 2 (n = 3) and one measurement is missing in temperature treatment 30.3 °C in week 2 (n = 4). Error bars indicate mean ± standard deviation. Significant differences are denoted by different letters ($p < 0.05$).

compared to 24.4 and 30.3 °C ($p = 0.001$ and $p = 0.002$, respectively; Supplementary Material Table S2). These findings were congruent with microscopy images showing visible signs of stress under the two most extreme temperature conditions. Stress was indicated by the retraction of algal endosymbionts as well as the occurrence of mottling at the end of the four-week experimental period (Fig. 4B, Supplementary Material Fig. S4). The other three treatments maintained an even yellow/brown coloration throughout the experiment.

In the light experiment, short term exposure to 25 and 37 µmol photons m^{-2} s^{-1} appeared to saturate electron transport rates, regardless of the light treatment in which individuals were acclimated, while 12.5 µmol photons m^{-2} s^{-1} (as used in the low light treatment) is clearly still in the sub-saturating range (Fig. 5, Supplementary Material Fig. S5). Regarding the shape of the photosynthesis-irradiance curves, optimal light intensity increased with increasing light levels, indicative of light acclimatization (Fig. 6; Linear mixed model, Effect of Light intensity: p

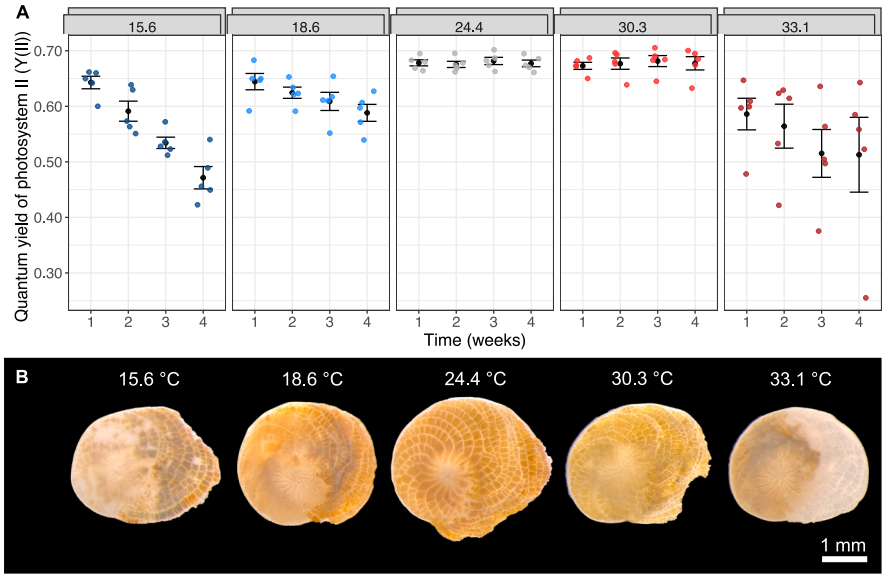

Fig. 4. Photosymbiont performance in the temperature experiment. A) Mean effective quantum yield of PSII ± standard deviation is shown for each temperature treatment over the course of the experiment. B) Representative microscopy images of an individual from each of the five temperature treatments at week 4 of the experiment. Patches of mottling were observed in the lowest temperature treatment whereas symbionts are retracted in the highest temperature treatment exposing the white calcareous test.

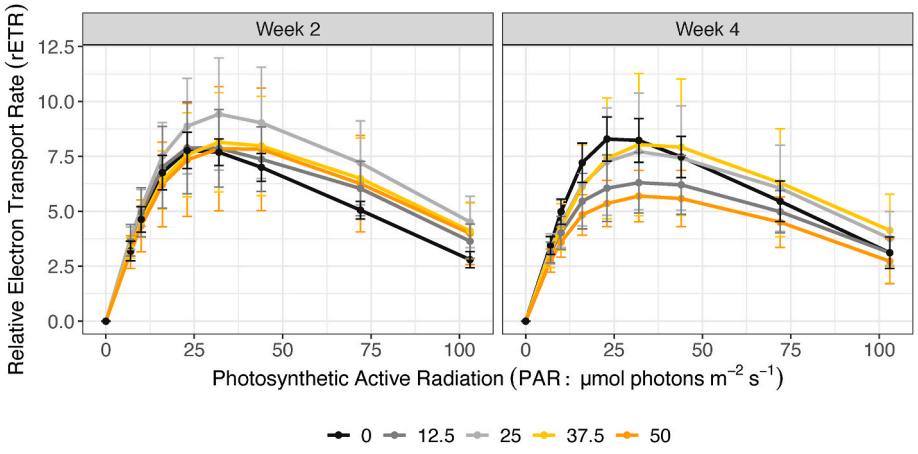

Fig. 5. Rapid light curves of LBF. The values of relative electron transport rate with their standard deviations are shown for each of the nine light levels for light curves acquired in week 2 and 4 of the light experiment.

< 0.001, $F(4,20) = 19.649$). However, the effect of light intensity on the initial slope (Linear mixed model, Effect of Light intensity: $p = 0.005$, $F(4,20) = 5.112$) was restricted to a lower slope in darkness compared to all light levels (Supplementary Material Fig. S6). The dark treatment further differed from the light treatments, with a significantly higher minimum saturation constant compared to the 12.5 and 25 µmol photons m^{-2} s^{-1} treatment ($p < 0.001$ and $p = 0.007$, respectively). Apart from the dark treatment, the minimum saturation constant was lower during growth at low light intensity (12 µmol photons m^{-2} s^{-1}) compared to all other light conditions (Supplementary Material Fig. S6 and Table S3).

3.4. Pigment analysis

Chl *a* concentrations showed an increasing trend from 50 to 12.5 µmol photons m^{-2} s^{-1}, but also large variability within treatments and no significant differences among them (Fig. 7). Ratios of Violaxanthin: Chl *a* concentrations increased with increasing light intensity and were significantly higher in 50 µmol photons m^{-2} s^{-1} than in 0 and 12.5 µmol photons m^{-2} s^{-1} (Tukey-Kramer, $p = 0.01$). While also diatoxanthin:Chl showed an increasing trend with increasing light levels, no significant differences were found in diatoxanthin and diadinoxanthin across the light treatments. Additional photosynthetic pigments (chlorophyll *c*3, chlorophyll *c*2, fucoxanthin, B-carotene and pheophytin a) did not show differences across the light treatments (Supplementary Material Fig. S7).

4. Discussion

Large benthic foraminifera play an important role in the global carbon cycle especially on reef ecosystems (Langer et al., 1997; Langer, 2008), but are sensitive to ongoing environmental changes caused by anthropogenic activities (e.g., Doo et al., 2014). While our results show survival of *H. depressa* at temperatures below their ambient temperature (Janse et al., 2008), physiological responses were compromised during both heat and cold stress confirming our first hypothesis. Our results further confirm relatively low light requirements of *H. depressa* (Röttger

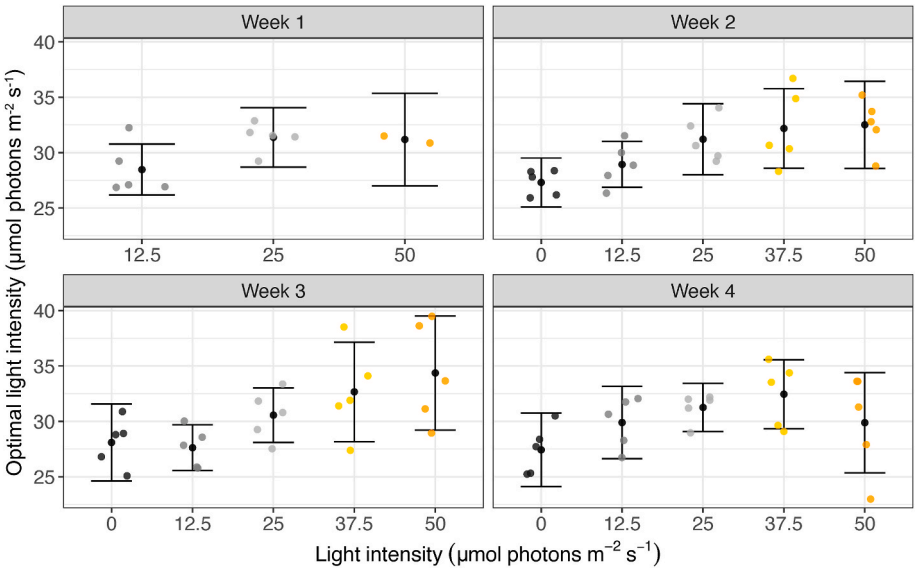

Fig. 6. Optimal light intensity derived from the rapid light curves (RLCs) under different growth light intensities. The mean ± standard deviation is shown.

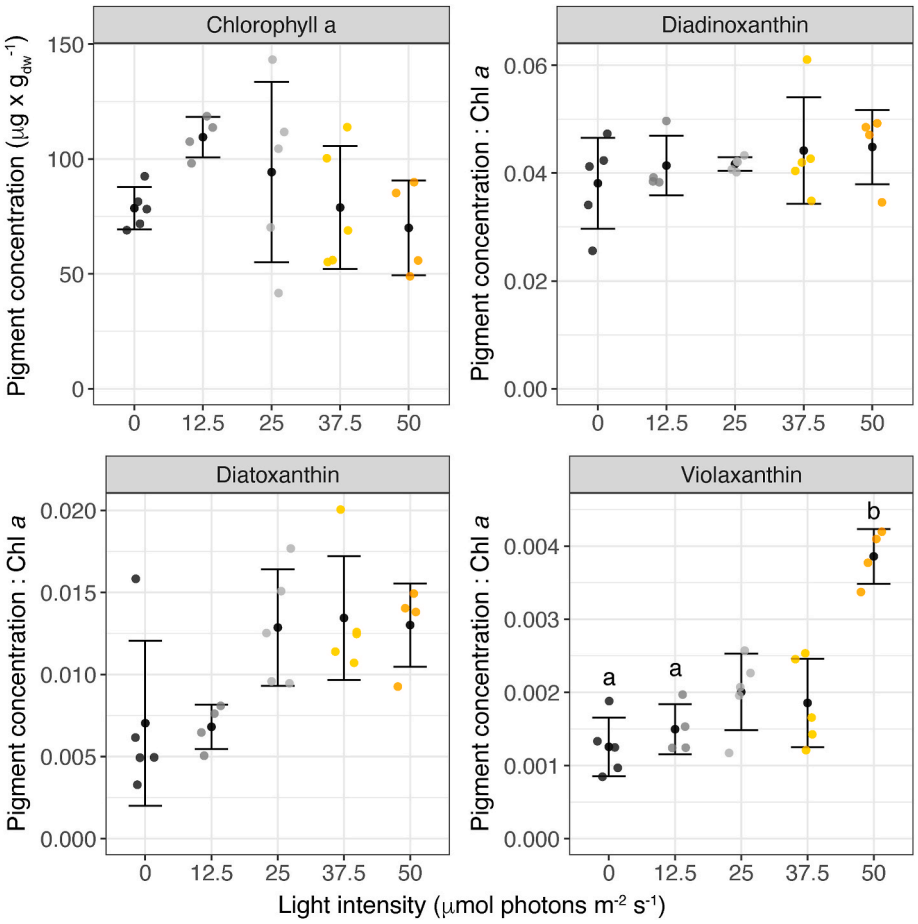

Fig. 7. Foraminiferal pigment content at the end of the experiment. Accessory pigments are expressed as weight-based ratios relative to chlorophyll *a*. The mean ± standard deviation is shown. Significant differences are indicated by different letters (p value < 0.05).

et al., 1980). Finally, we introduce micro-CT scanning of live foraminifera as a novel approach to quantify growth during experimental incubations. Together these results provide insights into the ecological adaptability and potential vulnerabilities of *H. depressa*, while opening new possibilities for further characterizing the physiology of foraminifera experimentally.

4.1. Methodological considerations

In order to quantify responses of foraminifera to environmental

conditions a solid measure of their performance is crucial, however there currently is no consensus about how to best measure foraminiferal growth. Dämmer et al. (2023) suggest the use of shell-based parameters, such as shell volume, shell density and chamber addition, directly to estimate calcification in foraminifera rather than using the total alkalinity technique. Existing methodologies allow visualization of newly formed chambers via calcein staining (Bernhard et al., 2004), or detailed assessment of shell morphology by micro-CT scanning (Prazeres and Pandolfi, 2016). Here we introduced micro-CT scanning of live foraminiferal specimens at the start and end of the experiment to track their calcification. Their survival and maintenance of a high photosynthetic yield suggests that foraminifera underwent the scanning procedure without compromising their health and thus being suitable to assess impact of temperature and light treatments on shell growth. Further refinement of live micro-CT scanning could optimize the resolution of the measurement relative to the stress experienced by the specimens and might offer additional information, such as the number of added chambers over time and changes in shell density to gain more insight into foraminiferal growth. While the alkalinity anomaly technique and the micro-CT scanning showed similar trends and overall low growth rates, the alkalinity anomaly technique resulted in more negative values compared to the micro-CT scanning. This discrepancy is likely caused by the lower sensitivity of alkalinity measurements and correction for changes in nutrient concentration based on assumptions about their uptake.

4.2. The thermal niche of H. depressa

This study showed an optimum temperature range between 24.4 °C and 30.3 °C for *H. depressa* based on photosynthetic activity, which indicates a degree of thermal flexibility and adaptability within its habitat. However, in terms of growth and calcification 24.4 °C appeared more favorable than 30.3 °C, as this was the only temperature at which positive growth rates were reached. Nevertheless, growth and calcification did not differ significantly between these two temperatures, and the optimum might lie in between. In any case, outside of this temperature range functioning becomes significantly compromised as shown by a decrease in growth, calcification, and quantum yield of photosystem II, as well as bleaching and/or mottling observed at 15.6 °C and 33.1 °C. While the decline in photosynthetic yield seemed already observable within the first week (Fig. 4), we note that the temporal sequence is difficult to interpret, as our acclimatization procedure and hence the first stress to specimens exposed to extreme temperatures already started prior to the final treatment temperatures being reached. Nevertheless, the decreased performance at the extreme temperatures is in line with our hypothesis that *H. depressa* is vulnerable to both heat and cold stress as their physiological functioning was impaired. This indicates a similar temperature optimum of 25 °C as observed for shell volume growth and calcification in the LBF *Sorites orbiculus* and *Amphistegina lobifera* (Kinoshita et al., 2021; Titelboim et al., 2021), but a slightly narrower thermal niche in our experimental system than could be expected based on the distribution range of *H. depressa*, which extends into waters of 33 °C (Langer and Hottinger, 2000). *H. depressa* generally live at the intermediate photic zone, however we do find some specimens at 5–15 m depth. Specimens occupying shallower depths might suffer more strongly from temperature stress (Sannassy Pilly et al., 2024; Giraldo-Ospina et al., 2020).

The response of *H. depressa* to high temperatures with moderate performance at 30.3 °C but strong decrease in photosynthetic efficiency at the highest temperature (33.1 °C) agrees with previous research (e.g. Schmidt et al., 2011). Negative effects of elevated temperatures (31.0 °C) on growth rate and photophysiology of *H. depressa* had been observed compared to a 28 °C control treatment (Schmidt et al., 2014), while bleaching only started to occur at 32 °C and 33 °C (Schmidt et al., 2011), and exposure to 34 °C was lethal to *H. depressa* within 96 h of exposure (van Dam et al., 2012). This temperature range over which a shift from healthy physiological performance to extreme heat-stress and bleaching occurs, is in line with the right-skewed shape of thermal niches and hence rapid declines in performance with warming beyond the thermal optimum (Rezende and Bozinovic, 2019). Due to this steep decline in performance, small, individual level differences in the shape of the thermal niche can cause relatively large differences in performance, as observed in the high variability in photosynthetic efficiency at the highest temperature treatment. At 33.1 °C effective quantum yield decreased overall, but standard error increased, thus indicating differences in response to high temperatures between specimens. In contrast, the decline in physiological performance towards lower temperatures is typically less steep, and despite a decline in photosynthetic efficiency of *H. depressa*'s endosymbionts observed towards the lower end of the thermal margin, less variability was observed at 15.6 °C. Whether this aligns with generally higher survival of *H. depressa* at low temperatures or an even lower minimum temperature at which *H. depressa* can photosynthesize will need to be resolved in future experiments.

In contrast to the maintenance of photosynthetic activity, positive rates of growth and calcification were only observed at the optimum temperature. Furthermore, a trend of a higher proportion of broken shells at the extreme temperatures as well as at 18.6 °C suggests a heightened fragility of the $CaCO_3$ shell at the edges of the optimal temperature range. Dissolution of $CaCO_3$ as detected by the alkalinity anomaly technique likely resulted in thinning of the shell, which provides a plausible explanation for the shell fragility observed at all temperatures except the control of 24.4 °C. All specimens were handled the same way throughout the experiment, ruling out handling as a contributing factor to the observed breakage patterns. These findings are in concordance with a previous study that showed a decrease in shell size and density for offshore populations of *A. lobifera* under elevated temperatures (Prazeres and Pandolfi, 2016), while our findings suggest the same to occur upon exposure to low temperatures. Although activity of the photosynthetic endosymbionts could be maintained over a relatively broad temperature range, the thermal range at which individuals and populations can grow and thrive is thus much narrower than the range that can be survived for a limited duration.

4.3. Light requirements for H. depressa growth and calcification

Growth rates of *H. depressa* were significantly reduced in darkness compared to all light levels tested, consistent with previous findings (Röttger et al., 1980) and supporting the light-enhanced calcification theory (Chalker and Taylor, 1975). Under these conditions, the light utilization efficiency decreased in *H. depressa* as reflected by higher E_K values in the dark compared to 12.5 μmol photons m^{-2} s^{-1}. Since investment into photosynthesis is no longer beneficial under darkness, resources might be shunted away from the endosymbiotic algae under these conditions. Nevertheless, some individuals still displayed growth in darkness, which might be explained by the presence of food in their surroundings. In this study, the seawater was supplemented with dried algae to mimic *in situ* conditions, since LBF have access to benthic algae in their natural environment (Topping et al., 2006). When exposed to dark conditions, LBF can rely more on heterotrophy (Lintner et al., 2023), which might have facilitated survival of *H. depressa* even in the absence of light.

While *H. depressa* can be found across a wide depth range with varying light intensities, it has a preference for low-light conditions (Hohenegger, 2000; Hohenegger et al., 2000; Nobes et al., 2008; Renema, 2018). The optimum light intensities of *H. depressa* based on rapid light curves (21–43 μmol photons m^{-2} s^{-1}) aligned well with those for rates of growth and calcification (25 and 37.5 μmol photons m^{-2} s^{-1}). While Nobes et al. (2008) showed higher growth rates and photosynthetic efficiency in foraminifera exposed to a natural daylight regime with an average of 30 μmol photons m^{-2} s^{-1} during the daylight hours compared to those exposed to an average of 113 and 418 μmol photons m^{-2} s^{-1}, the finer resolution of relatively low light intensities

assessed here allows us to determine a light optimum for growth between 20 and 40 μmol photons m^{-2} s^{-1}. This confirms our hypothesis that *H. depressa* has a low light optimum. While still able to survive relatively well in 50 μmol photons m^{-2} s^{-1} as reflected in robust growth and absence of bleaching, growth seemed to saturate or even slightly decline at this irradiance. The light optimum observed here is lower than observed in rapid light response curves for this species before (Nobes et al., 2008; Ziegler and Uthicke, 2011). This could be evidence that *H. depressa* is acclimatized to conditions at sample locations (Lee et al., 1989). At the collection depth in Burgers' Zoo, light levels ranged between 60 and 150 μmol photons m^{-2} s^{-1} at the rubble-water surface. However, specimens likely received less light due to their tendency to move towards cryptic microhabitats (Prazeres et al., 2016; Renema, 2018).

Photoacclimation was also observed over the course of the experiment, with rapid light curves showing an increase in the light optimum with growth under higher light intensities and the lowest half saturation being achieved during growth at the lowest light intensity. At the highest light intensity (50 μmol photons m^{-2} s^{-1}) the saturation of growth and photosynthesis coincided with first signs of photoprotection as seen in relatively higher violaxanthin concentrations and increasing trends in diadinoxanthin and diatoxanthin concentrations. The latter two constitute the xanthophyll cycle in diatoms that underlies their capability to adjust to rapid fluctuations in light intensity by dissipating excess light energy as heat via non-photochemical quenching (Lohr and Wilhelm, 1999; Blommaert et al., 2021). The role of violaxanthin in photoprotection is less clear in diatoms, although accumulation of violaxanthin-cycle pigments has been observed in diatoms under prolonged light stress, including evidence for xanthophyll cycle activity (Lohr and Wilhelm, 1999; Kuczynska et al., 2020). These photoacclimation strategies highlight the photosynthetic plasticity of the algal endosymbionts and likely act in concert with strategies employed by the host. LBF can for instance move in response to the light microenvironment (Petrou et al., 2017; Renema, 2018), and while this possibility was limited in our experiments some movement away from the light source was observed in the treatment with highest light intensity. Furthermore, adjustment of test thickness has been suggested to modulate light capture (Oron et al., 2018; Renema, 2018). Whether the lower rates of calcification observed in *H. depressa* under low light intensities simply represent the less favorable growth conditions, or also contribute to optimizing light capture cannot be resolved. In any case our results suggest that thinning of chambers results in a trade-off, because it increases the sensitivity to breakage, as reflected by the high number of broken individuals and the negative volume changes observed during growth in darkness. Overall, it is thus the close interplay between host and endosymbiont physiology and behavior that shapes the photoacclimation in LBF.

4.4. Interactive effects of multiple stressors on LBF physiology

Future climate conditions will result in multiple environmental factors changing in concert and the interactive effects of these are difficult to predict. Although not addressed directly in our experiments, such interactive effects might still influence experimental results, as responses to experimental manipulations will depend on the level of other environmental factors. For instance our light experiment revealed that the temperature experiment had been performed at a sub-optimal light level, potentially explaining the relatively low growth rates as well as the high level of shell breakage. Additionally, the relatively low pH of the aquarium water (pH 7.9) used for the experiments might further have contributed to these results. *Heterostegina depressa* thrives in the aquaria with low pH from which both specimens and water were collected. However, low pH can cause reduced calcification rates and thinner or lower density shells, i.e more fragile shells in symbiotic foraminifera (Prazeres et al., 2015). This may have been compensated for by the higher rates of calcification in the treatments with less breakage. In hindsight the addition of dried algae as food might also have supported bacterial growth and respiration leading to a further decrease in pH and negative impacts on calcification. However, many unknowns remain about the interactive effects of carbonate chemistry and food availability, with the primary factors temperature and light assessed in our experiments.

LBF are projected to experience both larger fluctuations in light levels as well as elevations in sea surface temperatures, resulting in a shift in their species distribution towards cooler subtropical regions (Titelboim et al., 2021). But due to temperature sensitivity, cold stress could be a limiting factor to range expansion of tropical LBF (Langer and Hottinger, 2000; Vergés et al., 2014). Hence, broad thermal tolerance is crucial for species to thrive after migration to mid-latitudes. Our results suggest that *H. depressa* survival might be compromised following a shift in species distribution. Winter temperatures at mid-latitude habitats in the Mediterranean can reach to 9.7–17.7 °C depending on the region (Shaltout and Omstedt, 2014), the upper range of which *H. depressa* can survive based on our experiments. *H. depressa* has already invaded the south-eastern Mediterranean through the Suez Canal, which forms a suitable habitat due to its high winter temperatures, high salinity and oligotrophic environment (Langer and Hottinger, 2000; Stulpinaite et al., 2020). However, LBF performance in a new habitat will depend on interactive effects of many abiotic factors as well as biotic interactions within the community, making predictions based on single-factor experiments as performed here very challenging. The temperature niche of *H. depressa* might thus be broader for growth at optimum light and pH, while also the optima themselves might shift with changes in other environmental factors. For instance, organisms living in turbid ecosystems, where light intensities are generally lower, can show tolerance to higher water temperatures and therefore resist bleaching to a certain degree (Rosedy et al., 2023). Future comparative studies that target the interactive effects of temperature and light with other environmental variables will be of utmost relevance as results may show different physiological responses and eventual tolerance to more extreme environments.

CRediT authorship contribution statement

Chiara M. Duijser: Writing – original draft, Visualization, Investigation, Formal analysis, Conceptualization. **Rebecca S. van Oostveen:** Writing – original draft, Visualization, Investigation, Formal analysis, Conceptualization. **Elsa B. Girard:** Writing – review & editing, Visualization, Conceptualization. **Willem Renema:** Writing – review & editing, Funding acquisition, Conceptualization. **Susanne Wilken:** Writing – review & editing, Supervision, Funding acquisition, Conceptualization.

Funding

This work was partly funded by the European Union's Horizon 2020 research and innovation program under the Marie Skłodowska-Curie grant agreement (4D-REEF, No 813360) to WR and a Vidi grant (no 193.101) from the Dutch Research Council (NWO) to SW.

Declaration of competing interest

The authors declare that they have no known competing financial interests or personal relationships that could have appeared to influence the work reported in this paper.

Acknowledgements

This project would not have been possible without the support of Max Janse from Burger's Zoo by providing the foraminifera specimens. We would like to also thank Rob Langelaan for his help with the micro-CT scanning procedure at Naturalis Biodiversity Center in Leiden, Bas

van Beusekom for his technical advice and help with building the experimental set-up and Pieter Slot for running the nutrient analysis at the University of Amsterdam.

Appendix A. Supplementary data

Supplementary data to this article can be found online at https://doi.org/10.1016/j.ecss.2024.109075.

Data availability

I have shared the link to my data at the attach file step.

Light and temperature niches of the large benthic foraminifer Heterostegina depressa (Original data) (Figshare)

References

Baker, A.C., Glynn, P.W., Riegl, B., 2008. Climate change and coral reef bleaching: an ecological assessment of long-term impacts, recovery trends and future outlook. Estuar. Coast Shelf Sci. 80 (4), 435–471. https://doi.org/10.1016/j.ecss.2008.09.003.

Benjamini, Y., Hochberg, Y., 1995. Controlling the false discovery rate: a practical and powerful approach to multiple testing. J. Roy. Stat. Soc. B 57 (1), 289–300. https://doi.org/10.1111/j.2517-6161.1995.tb02031.x.

Bernhard, J.M., Blanks, J.K., Hintz, C.J., Chandler, G.T., 2004. Use of the fluorescent calcite marker calcein to label foraminiferal tests. J. Foraminifer. Res. 34 (2), 96–101. https://doi.org/10.2113/0340096.

Blommaert, L., Chafai, L., Bailleul, B., 2021. The fine-tuning of NPQ in diatoms relies on the regulation of both xanthophyll cycle enzymes. Sci. Rep. 11 (1), 1–16. https://doi.org/10.1038/s41598-021-91483-x.

Chalker, B.E., Taylor, D.L., 1975. Light-enhanced calcification, and the role of oxidative phosphorylation in calcification of the coral *Acropora cervicornis*. Proc. Roy. Soc. Lond. B. 190, 323–331.

van Dam, J.W., Negri, A.P., Mueller, J.F., Altenburger, R., Uthicke, S., 2012. Additive pressures of elevated sea surface temperatures and herbicides on symbiont-bearing foraminifera. PLoS One 7 (3), e33900. https://doi.org/10.1371/journal.pone.0033900.

Dämmer, L.K., Ivkić, A., De Nooijer, L., Renema, W., Webb, A.E., Reichart, G.-J., 2023. Impact of dissolved CO_2 on calcification in two large, benthic foraminiferal species. PLoS One 18 (8), e0289122. https://doi.org/10.1371/journal.pone.0289122.

Dawson, J.L., Smithers, S.G., Hua, Q., 2014. The importance of large benthic foraminifera to reef island sediment budget and dynamics at Raine Island, northern Great Barrier Reef. Geomorphology 222, 68–81. https://doi.org/10.1016/j.geomorph.2014.03.023.

Doo, S.S., Hamylton, S., Byrne, M., 2012. Reef-scale assessment of intertidal large benthic foraminifera populations on One Tree Island, Great Barrier Reef and their future carbonate production potential in a warming ocean. Zool. Stud. 51 (8), 1298–1307.

Doo, S.S., Fujita, K., Byrne, M., Uthicke, S., 2014. Fate of calcifying tropical symbiont-bearing large benthic foraminifera: living sands in a changing ocean. Biol. Bull. 226 (3), 169–186. https://doi.org/10.1086/BBLv226n3p169.

Duguay, L.E., Taylor, D.L., 1978. Primary production and calcification by the soritid foraminifer *Archais angulatus* (Fichtel & Moll). J. Protozool. 25 (3), 356–361. https://doi.org/10.1111/j.1550-7408.1978.tb03903.x.

Dunn, O.J., 1964. Multiple comparisons using rank sums. Technometrics 6 (3), 241–252.

Eilers, P.H.C., Peeters, J.C.H., 1988. A model for the relationship between light intensity and the rate of photosynthesis in phytoplankton. Ecol. Model. 42 (3–4), 199–215.

Faber, W.W., Lee, J.J., 1991. Histochemical evidence for digestion in *Heterostegina depressa* and *Operculina ammonoides* (Foraminifera). Endocytobiology and Cell Research 8, 53–59.

Fujita, K., Okai, T., Hosono, T., 2014. Oxygen metabolic responses of three species of large benthic foraminifers with algal symbionts to temperature stress. PLoS One 9 (3), e90304. https://doi.org/10.1371/journal.pone.0090304.

Genty, B., Briantais, J.-M., Baker, N.R., 1989. The relationship between the quantum yield of photosynthetic electron transport and quenching of chlorophyll fluorescence. Biochim. Biophys. Acta Gen. Subj. 990 (1), 87–92. https://doi.org/10.1016/S0304-4165(89)80016-9.

Giraldo-Ospina, A., Kendrick, G.A., Hovey, R.K., 2020. Depth moderates loss of marine foundation species after an extreme marine heatwave: could deep temperate reefs act as a refuge? Proc. Biol. Sci. 287 (1928), 20200709. https://doi.org/10.1098/rspb.2020.0709.

Girard, E.B., Ferse, S., Ambo-Rappe, R., Jompa, J., Renema, W., 2022. Dynamics of large benthic foraminiferal assemblages: a tool to foreshadow reef degradation? Sci. Total Environ. 811, 151396. https://doi.org/10.1016/j.scitotenv.2021.151396.

Hallock, P., 1981. Algal symbiosis: a mathematical analysis. Mar. Biol. 62, 249–255.

Hallock, P., 1985. Why are larger Foraminifera large? Paleobiology 11 (2), 195–208. https://doi.org/10.1017/S0094837300011507.

Hallock, P., 2000. Symbiont-bearing foraminifera: harbingers of global change? Micropaleontology 46, 95–104.

Hallock, P., Lidz, B.H., Cockey-Burkhard, E.M., Donnelly, K.B., 2003. Foraminifera as bioindicators in coral reef assessment and monitoring: the FORAM index. Environ. Monit. Assess. 81 (1/3), 221–238. https://doi.org/10.1023/a:1021337310386.

Hallock, P., Williams, D.E., Fisher, E.M., Toler, S.K., 2006. Bleaching in Foraminifera with algal symbionts: implications for reed monitoring and risk assessment. Anuário do Instituto de Geosciências 29 (1), 108–129. https://doi.org/10.11137/2006_1_108-128.

Hohenegger, J., 2000. Coenoclines of larger foraminifera. Micropaleontology 46, 127–151.

Hohenegger, J., 2006. The importance of symbiont-bearing benthic foraminifera for West Pacific carbonate beach environments. Mar. Micropaleontol. 61 (1–3), 4–39. https://doi.org/10.1016/j.marmicro.2006.05.007.

Hohenegger, J., Yordanova, E., Hatta, A., 2000. Remarks on west pacific nummulitidae (foraminifera). J. Foraminifer. Res. 30 (1), 3–28. https://doi.org/10.2113/0300003.

Janse, M., Wensing, J., Gieling, H., de Jongh, T., Leewis, R., 2008. Ecological management of a large coral reef eco-display at Burgers zoo, arnhem, The Netherlands. Advances in coral husbandry in public aquariums. In: Leewis, R.J., Janse, M. (Eds.), Public Aquarium Husbandry Series. Arnhem: Burgers Zoo), pp. 293–303.

Kassambara, A., 2020. rstatix: pipe-friendly framework for basic statistical tests. R package version 0.5.0. https://CRAN.R-project.org/package=rstatix.

Kinoshita, S., Kuroyanagi, A., Kawahata, H., Fujita, K., Ishimura, T., Suzuki, A., Sasaki, O., Nishi, H., 2021. Temperature effects on the shell growth of a larger benthic foraminifer (*Sorites orbiculus*): results from culture experiments and micro X-ray computed tomography. Mar. Micropaleontol. 163, 101960. https://doi.org/10.1016/j.marmicro.2021.101960.

Kuczynska, P., Jemiola-Rzeminska, M., Nowicka, B., Jakubowska, A., Strzalka, W., Burda, K., Strzalka, K., 2020. The xanthophyll cycle in diatom *Phaeodactylum tricornutum* in response to light stress. Plant Physiol. Biochem. 152, 125–137. https://doi.org/10.1016/j.plaphy.2020.04.043.

ter Kuile, B.H., Erez, J., 1991. Carbon budgets for two species of benthonic symbiont-bearing foraminifera. Biol. Bull. 180 (3), 489–495. https://doi.org/10.2307/1542350.

ter Kuile, B.H., Erez, J., Lee, J.J., 1987. The role of feeding in the metabolism of larger symbiont bearing Foraminifera. Symbiosis 4, 335–336.

Langer, M.R., 2008. Assessing the contribution of foraminiferan protists to global ocean carbonate production. J. Eukaryot. Microbiol. 55 (3), 163–169. https://doi.org/10.1111/j.1550-7408.2008.00321.x.

Langer, M.R., Hottinger, L., 2000. Biogeography of selected "larger" foraminifera. Micropaleontology 46, 105–126.

Langer, M.R., Silk, M.T., Lipps, J.H., 1997. Global ocean carbonate and carbon dioxide production; the role of reef Foraminifera. J. Foraminifer. Res. 27 (4), 271–277. https://doi.org/10.2113/gsjfr.27.4.271.

Lee, J.J., 2006. Algal symbiosis in larger foraminifera. Symbiosis 42, 63–75.

Lee, J.J., Anderson, O.R., 1991. Biology of Foraminifera. Academic Press, London.

Lee, J.J., McEnery, M.E., Kuile, B.T., Erez, J., Röttger, R., Rockwell, R.F., Faber Jr, W.W., Lagziel, A., 1989. Identification and distribution of endosymbiotic diatoms in larger foraminifera. Micropaleontology 35 (4), 353–366. https://doi.org/10.2307/1485677.

Lintner, M., Lintner, B., Schagerl, M., Wanek, W., Heinz, P., 2023. The change in metabolic activity of a large benthic foraminifera as a function of light supply. Sci. Rep. 13 (1), 8240. https://doi.org/10.1038/s41598-023-35342-x.

Lohr, M., Wilhelm, C., 1999. Algae displaying the diadinoxanthin cycle also possess the violaxanthin cycle. Proc. Natl. Acad. Sci. USA 96 (15), 8784–8789. https://doi.org/10.1073/pnas.96.15.8784.

Mair, P., Wilcox, R.R., 2020. Robust statistical methods in R using the WRS2 Package. Behav. Res. Methods 52, 464–488.

Mantzouki, E., Lürling, M., Fastner, J., de Senerpont Domis, L., Wilk-Woźniak, E., Koreivienė, J., Seelen, L., Teurlincx, S., et al., 2018. Temperature effects explain continental scale distribution of cyanobacterial toxins. Toxins 10 (4), 156. https://doi.org/10.3390/toxins10040156.

McConnaughey, T.A., Whelan, J.F., 1997. Calcification generates protons for nutrient and bicarbonate uptake. Earth Sci. Rev. 42 (1), 95–117. https://doi.org/10.1016/S0012-8252(96)00036-0.

Nobes, K., Uthicke, S., Henderson, R., 2008. Is light the limiting factor for the distribution of benthic symbiont bearing foraminifera on the Great Barrier Reef? J. Exp. Mar. Biol. Ecol. 363 (1–2), 48–57. https://doi.org/10.1016/j.jembe.2008.06.015.

Oron, S., Abramovich, S., Almogi-Labin, A., Woeger, J., Erez, J., 2018. Depth related adaptations in symbiont bearing benthic foraminifera: new insights from a field experiment on *Operculina ammonoides*. Sci. Rep. 8 (1), 9560. https://doi.org/10.1038/s41598-018-27838-8.

Petrou, K., Ralph, P.J., Nielsen, D.A., 2017. A novel mechanism for host-mediated photoprotection in endosymbiotic foraminifera. ISME J. 11 (2), 453–462. https://doi.org/10.1038/ismej.2016.128.

Prazeres, M., Pandolfi, J.M., 2016. Effects of elevated temperature on the shell density of the large benthic Foraminifera *Amphistegina lobifera*. J. Eukaryot. Microbiol. 63 (6), 786–793. https://doi.org/10.1111/jeu.12325.

Prazeres, M., Renema, W., 2018. Evolutionary significance of the microbial assemblages of large benthic Foraminifera. Biol. Rev. 94 (3), 828–848. https://doi.org/10.1111/brv.12482.

Prazeres, M., Uthicke, S., Pandolfi, J.M., 2015. Ocean acidification induces biochemical and morphological changes in the calcification process of large benthic foraminifera. Proc. R. Soc. B: Biol. Sci. 282 (1803), 20142782.

Prazeres, M., Uthicke, S., Pandolfi, J., 2016. Changing light levels induce photo-oxidative stress and alterations in shell density of *Amphistegina lobifera* (Foraminifera). Mar. Ecol. Prog. Ser. 549, 69–78. https://doi.org/10.3354/meps11698.

Renema, W., 2018. Terrestrial influence as a key driver of spatial variability in large benthic foraminiferal assemblage composition in the Central Indo-Pacific. Earth Sci. Rev. 177, 514–544. https://doi.org/10.1016/j.earscirev.2017.12.013.

Reymond, C., Uthicke, S., Pandolfi, J., 2011. Inhibited growth in the photosymbiont-bearing foraminifer *Marginopora vertebralis* from the nearshore Great Barrier Reef, Australia. Mar. Ecol. Prog. Ser. 435, 97–109. https://doi.org/10.3354/meps09172.

Rezende, E.L., Bozinovic, F., 2019. Thermal performance across levels of biological organization. Phil. Trans. R. Soc. B 374, 10. https://doi.org/10.1098/rstb.2018.0549.

Rosedy, A., Ives, I., Waheed, Z., Hussein, M.A.S., Sosdian, S., Johnson, K., Santodomingo, N., 2023. Turbid reefs experience lower coral bleaching effects in NE Borneo (Sabah, Malaysia). Regional Studies in Marine Science 68, 103268. https://doi.org/10.1016/j.rsma.2023.103268.

Ross, B.J., Hallock, P., 2016. Dormancy in the foraminifera: a review. J. Foraminifer. Res. 46 (4), 358–368. https://doi.org/10.2113/gsjfr.46.4.358.

Röttger, R., Irwan, A., Schmaljohann, R., Franzisket, L., 1980. Growth of the symbiont-bearing foraminifera *Amphistegina lessonii* d'Orbigny and *Heterostegina depressa* d'Orbigny (protozoa). In: Schwemmler, W., Schenk, H.E.A. (Eds.), Endosymbiosis and Cell Biology. De Gruyter, Berlin, pp. 125–132. https://doi.org/10.1515/9783111385068-015.

RStudio Team, 2020. RStudio. Integrated Development for R. RStudio, PBC, Boston, MA. http://www.rstudio.com/.

Sannassy Pilly, S., Roche, R.C., Richardson, L.E., Turner, J.R., 2024. Depth variation in benthic community response to repeated marine heatwaves on remote Central Indian Ocean reefs. R. Soc. Open Sci. 11 (3), 231246. https://doi.org/10.1098/rsos.231246.

Schmidt, C., Heinz, P., Kucera, M., Uthicke, S., 2011. Temperature-induced stress leads to bleaching in larger benthic foraminifera hosting endosymbiotic diatoms. Limnol. Oceanogr. 56 (5), 1587–1602. https://doi.org/10.4319/lo.2011.56.5.1587.

Schmidt, C., Kucera, M., Uthicke, S., 2014. Combined effects of warming and ocean acidification on coral reef Foraminifera *Marginopora vertebralis* and *Heterostegina depressa*. Coral Reefs 33 (3), 805–818. https://doi.org/10.1007/s00338-014-1151-4.

Schmidt, C., Titelboim, D., Brandt, J., Herut, B., Abramovich, S., Almogi-Labin, A., Kucera, M., 2016. Extremely heat tolerant photo-symbiosis in a shallow marine benthic foraminifera. Sci. Rep. 6 (1), 30930. https://doi.org/10.1038/srep30930.

Shaltout, M., Omstedt, A., 2014. Recent sea surface temperature trends and future scenarios for the Mediterranean Sea. Oceanologia 56 (3), 411–443. https://doi.org/10.5697/oc.56-3.411.

Smith, S.V., Key, G.S., 1975. Carbon dioxide and metabolism in marine environments. Limnol. Oceanogr. 20 (3), 493–495. https://doi.org/10.4319/lo.1975.20.3.0493.

Smith, S.V., Kinsey, D.W., 1978. Calcification and organic carbon metabolism as indicated by carbon dioxide. In: Stoddart, D.R., Johannes, R.E. (Eds.), Coral Reefs: Research Methods. UNESCO, Monographs on Oceanographic Methodology No. 5, Paris, pp. 469–484.

van der Staay, G.W., Brouwer, A., Baard, R.L., van Mourik, F., Matthijs, H.C., 1992. Separation of photosystems I and II from the oxychlorobacterium (prochlorophyte) *Prochlorothrix hollandica* and association of chlorophyll b binding antennae with photosystem II. Biochim. Biophys. Acta Bioenerg. 1102 (2), 220–228. https://doi.org/10.1016/0005-2728(92)90103-9.

Stulpinaite, R., Hyams-Kaphzan, O., Langer, M.R., 2020. Alien and cryptogenic foraminifera in the mediterranean sea: a revision of taxa as part of the eu 2020 marine strategy framework directive. Mediterr. Mar. Sci. 21 (3), 719–758. https://doi.org/10.12681/mms.24673.

Titelboim, D., Thangarjan, S., Raposo, D., Morard, R., Kucera, M., Ashckenazi-Polivoda, S., Almogi-Labin, A., Herut, B., Manda, S., Abramovich, S., Gold, D.A., Abdu, U., 2021. The transcriptomic signature of cold and heat stress in benthic foraminifera—implications for range expansions of marine calcifiers. Funct. Ecol. 35 (12), 2679–2690. https://doi.org/10.1111/1365-2435.13929.

Topping, J.N., Murray, J.W., Pond, D.W., 2006. Sewage effects on the food sources and diet of benthic foraminifera living in oxic sediment: a microcosm experiment. J. Exp. Mar. Biol. Ecol. 329 (2), 239–250. https://doi.org/10.1016/j.jembe.2005.09.013.

Uthicke, S., Vogel, N., Doyle, J., Schmidt, C., Humphrey, C., 2012. Interactive effects of climate change and eutrophication on the dinoflagellate-bearing benthic foraminifer *Marginopora vertebralis*. Coral Reefs 31 (2), 401–414. https://doi.org/10.1007/s00338-011-0851-2.

Vergés, A., Steinberg, P.D., Hay, M.E., Poore, A.G.B., Campbell, A.H., Ballesteros, E., Heck, K.L., Booth, D.J., Coleman, M.A., Feary, D.A., et al., 2014. The tropicalization of temperate marine ecosystems: climate-mediated changes in herbivory and community phase shifts. Proc. Biol. Sci. 281 (1789), 20140846. https://doi.org/10.1098/rspb.2014.0846.

Weinmann, A.E., Rödder, D., Lötters, S., Langer, M.R., 2013. Heading for new shores: projecting marine distribution ranges of selected larger foraminifera. PLoS One 8 (4), e62182. https://doi.org/10.1371/journal.pone.0062182.

Wickham, H., 2009. ggplot2: Elegant Graphics for Data Analysis. Springer, New York.

Wild, C., Hoegh-Guldberg, O., Naumann, M.S., Colombo-Pallotta, M.F., Ateweberhan, M., Fitt, W.K., Iglesias-Prieto, R., Palmer, C., Bythell, J.C., Ortiz, J.-C., Loya, Y., Van Woesik, R., 2011. Climate change impedes scleractinian corals as primary reef ecosystem engineers. Mar. Freshw. Res. 62 (2), 205–215. https://doi.org/10.1071/MF10254.

Wilken, S., Schuurman, J.M., Matthijs, H.C.P., 2014. Do mixotrophs grow as photoheterotrophs? Photophysiological acclimation of the chrysophyte *Ochromonas danica* after feeding. New Phytol. 204 (4), 882–889. https://doi.org/10.1111/nph.12975.

Wolf-Gladrow, D.A., Zeebe, R.E., Klaas, C., Körtzinger, A., Dickson, A.G., 2007. Total alkalinity: the explicit conservative expression and its application to biogeochemical processes. Mar. Chem. 106 (1–2), 287–300. https://doi.org/10.1016/j.marchem.2007.01.006.

Yamano, H., Miyajima, T., Koike, I., 2000. Importance of foraminifera for the formation and maintenance of a coral sand cay: green Island, Australia. Coral Reefs 19 (1), 51–58. https://doi.org/10.1007/s003380050226.

Zeebe, R.E., Wolf-Gladrow, D., 2001. CO_2 in Seawater: Equilibrium, Kinetics, Isotopes. Elsevier Oceanography Series 65, Elsevier, Amsterdam.

Ziegler, M., Uthicke, S., 2011. Photosynthetic plasticity of endosymbionts in larger benthic coral reef Foraminifera. J. Exp. Mar. Biol. Ecol. 407 (1), 70–80. https://doi.org/10.1016/j.jembe.2011.07.009.